The Effect of Ceramic Reinforcements during Spray Atomization and Codeposition of Metal Matrix Composites: Part II. Solid-State Cooling Effects

MANOJ GUPTA, FARGHALLI MOHAMED, and ENRIQUE LAVERNIA

In the present study, the mechanisms governing the evolution of microstructure during spray atomization and codeposition of metal matrix composites (MMCs) were investigated, with particular emphasis on the effects of the ceramic phase on the resulting microstructure during solid-state cooling. The grain size refinement that is commonly observed when a distribution of ceramic particulates is coinjected into a metallic spray during spray atomization and deposition processing was rationalized in terms of three distinct effects: (a) solidification effects, (b) heat-transfer effects, and (c) solid-state cooling effects. The solidification and heat-transfer effects were discussed in Part I.[1] Regarding solid-state cooling effects, the present results show that the presence of a dispersion of ceramic particulates in the aluminum matrix effectively reduces the rate of grain growth during solid-state cooling. Experimental support to this suggestion was provided by the results of an investigation on the changes in grain size following isochronal thermal anneals.

I. INTRODUCTION

In Part I,[1] the authors showed that the coinjection of ceramic particulates during spray atomization and codeposition promotes a reduction in grain size. In order to provide insight into the effects of the ceramic particulates on microstructural evolution, a model was formulated[1] to account for the transfer of thermal energy from the atomized matrix to the ceramic particulates during two stages: (a) atomization and (b) deposition. The numerical results obtained using SiC particulates in an aluminum matrix show that 10 pct of the enthalpy of the atomized spray is transferred to ceramic particulates during atomization, whereas 10 pct of the thermal energy available after deposition will be consumed in the process of equilibrating the temperature of the particulates to that of the matrix. In addition, solidification effects were also considered,[2] although a thorough study of this phenomenon was outside of the scope of the work.

In the present study, the effects of SiC on the microstructure during solid-state cooling (*e.g.*, after the matrix/particulate mixture has arrived on the substrate) were investigated, with particular emphasis on the rate of grain growth. To identify the role of SiC during grain boundary migration, the reinforced and unreinforced materials were exposed to various isothermal heat treatments.

II. EXPERIMENTAL

The details of the processing and the microstructural analysis were described in Part I;[1] other relevant details are given below.

A. *Thermomechanical Treatment*

Following spray atomization and codeposition, thermal treatment was conducted on as-spray deposited and spray deposited and hot extruded samples of reinforced and unreinforced Al-Li materials. The extrusion step was accomplished using an 82.7 MPa press at a temperature of 400 °C with an area reduction of 16:1. The extrusion step was used in the present study in order to close the micrometer size porosity normally associated with spray-atomized and -deposited materials.[3–10] Following spray atomization and codeposition, samples from experiments 1 and 2 were isochronally annealed at 400 °C and 600 °C for time intervals up to 100 minutes in order to study the effects of temperature and time on grain growth. In order to restore the grain size obtained after extrusion to that obtained immediately after spray deposition, as-spray deposited and hot extruded samples from experiments 1 and 2 were given a normalizing treatment, which consisted of thermal annealing at 400 °C for 30 and 40 minutes, respectively, before being annealed further at 400 °C and 600 °C. Finally, as-spray deposited samples from experiment 3 were annealed at 400 °C for 100 minutes in order to study the segregation of constituent elements and the presence of precipitated phases in regions adjacent to porosity.

B. *Scanning Electron Microscopy*

Scanning electron microscopy (SEM) studies were conducted using a HITACHI S-500 microscope. The samples were sectioned to a thickness of 0.5 cm and mirror polished using conventional techniques. The polished samples were then examined in secondary electron mode for microstructural details; point analysis was carried out at selected regions of the sample surface to detect the presence of constituent elements.

III. RESULTS

A. *Microstructural Characterization*

In order to characterize the size, distribution, and location of SiC particulates in the Al-Li matrix, image analysis was conducted on a number of samples taken from experiment 2. The size and distribution of the SiC

MANOJ GUPTA, Graduate Student, FARGHALLI MOHAMED, Professor, and ENRIQUE LAVERNIA, Associate Professor of Materials Science and Engineering, are with the Department of Mechanical and Aerospace Engineering, University of California, Irvine, CA 92717.

Manuscript submitted September 17, 1991.

particulates obtained from image analysis were then used to compute the SiC interparticulate spacing according to the formula discussed by Nardone and Prewo:[11]

$$\lambda = (lt/V_f)^{1/2} \quad [1]$$

where λ is the interparticulate spacing and t, l, and V_f are the thickness, length, and volume fraction of the SiC particulates, respectively. For the present case, the dimensions of SiC particulates are characterized by the equivalent diameter, d. The value of λ was calculated by assuming $l = t = d$;[12] this assumption is reasonable in view of the equiaxed geometry of the particulates. The results of the image analysis and the computed interparticulate spacings, λ, for experiment 2 are shown in Table I.

Scanning electron microscopy of samples removed from the central portion of the spray-deposited material from experiment 3 revealed the presence of a finite amount of unconnected porosity (Figure 1). The micron-sized pores were preferentially located at the grain boundaries and exhibited an irregular, faceted morphology. The distribution of pores in the as-spray deposited microstructure was found to be bimodal, with a large proportion of pores in the 1 to 2-μm and 6-μm size ranges. In addition, the results of the SEM also reveal the evidence of precipitation at the free surface of the porosity (Figure 2) in the as-spray deposited sample taken from experiment 3. The results of elemental point analyses conducted on the porosity and at 2 and 6 μm from the porosity after thermal exposure of the samples at 400 °C for 100 minutes are shown in Figure 3.

Metallographic analysis was conducted on coupons of the spray-deposited Al-Li, Al-Cu, Al-Li-SiC, and Al-Cu-SiC materials. The microscopy studies revealed the presence of equiaxed grains. This grain morphology has also been reported by other investigators.[13–21] It has been proposed[20] that the formation of an equiaxed grain morphology during spray deposition is a result of three simultaneous processes: (1) dendrite arm fragmentation, (2) nucleation/grain multiplication, and (3) constrained growth. During deposition, there is extensive fragmentation of the dendrite arms formed during solidification, as a result of the repeated impact of the partially solidified droplets, first with the deposition surface and, subsequently, with each other. More recently, in a study involving Ni_3Al powders, Liang and Lavernia[21] proposed that the formation of equiaxed grains from dendrites during annealing evolves from two distinct

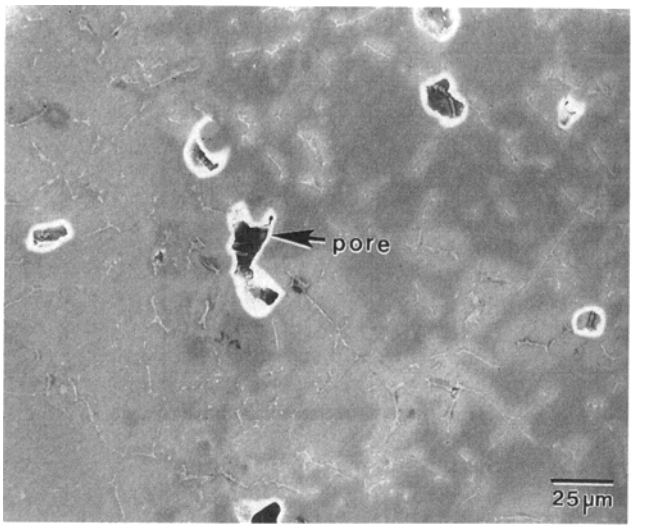

Fig. 1 — SEM micrograph showing the presence of unconnected porosity in the as-spray deposited sample taken from experiment 3.

mechanisms: (a) the coarsening of secondary dendrite arms and (b) the growth and coalescence of primary dendrite arms. Kinetic analyses of the experimental data showed that the activation energy necessary for grain growth to occur was higher than the activation energy for recrystallization but lower than the activation energy for diffusion.

B. *Grain Growth Behavior*

In order to provide insight into the effects of the SiC particulates on the microstructure during solid-state cooling, grain growth studies were conducted on the samples taken from experiments 1 and 2. The grain sizes were determined using the linear intercept method after isochronal anneals at 400 °C and 600 °C (Table II and Figure 4). The results of grain size measurements, shown in Figure 4, indicate a logarithmic trend of grain growth with time for both the Al-Li and Al-Li-SiC materials. Not unexpectedly, it can be seen that the rate of grain growth of the Al-Li-SiC material at 400 °C and 600 °C is lower than that of the Al-Li material. The microstructure of both the as-spray deposited binary Al-Li alloy and the SiC reinforced Al-Li alloy consisted of equiaxed

Table I. Results of Image Analysis of Al-Li-SiC Composite

Sample Number*	Equivalent Diameter (μm)**				Volume Fraction† (pct)				Interparticulate Spacing‡ (λ, μm)
	Minimum	Maximum	Mean	σ	Minimum	Maximum	Mean	σ	
2A	0.57	09.00	2.70	~2.01	1.92	08.33	3.49	1.82	14.48
2B	0.57	10.00	2.71	2.10	2.89	06.15	4.56	1.13	12.69
2C	0.57	12.00	2.10	1.76	4.40	13.44	7.89	1.91	07.48

*A, B, C designations refer to top, center, bottom regions, respectively, of the spray-deposited Al-Li-SiC.
**The equivalent diameter is a measure of the size of the SiC particulates.
†These values of the volume fraction were determined using quantitative metallography.
‡These values were computed from Eq. [1].

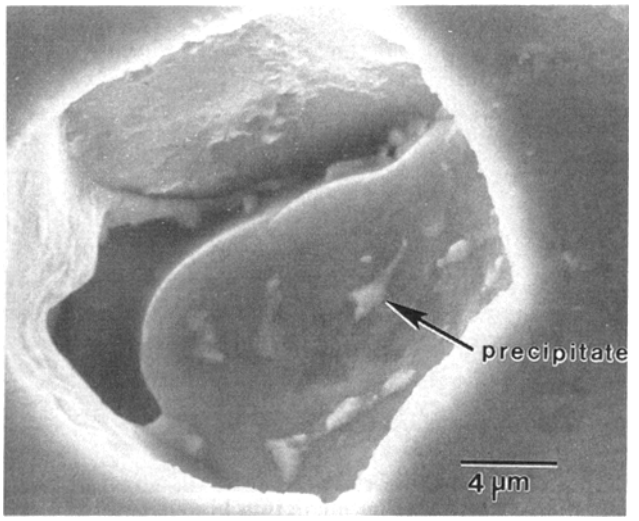

Fig. 2—SEM micrograph showing the evidence of precipitation at the free surface of the porosity in the as-spray deposited sample taken from experiment 3.

grains before and after the isochronal heat treatments (Figures 5 and 6).

The results of grain growth studies conducted on as-spray deposited and hot extruded samples of the Al-Li and Al-Li-SiC materials are summarized in Table III. The results presented in this table show that, at 400 °C, the rate of grain growth of the Al-Li-SiC material was higher than that observed for the Al-Li material, while this trend was reversed at 600 °C. It is worthwhile noting that the as-spray deposited and hot extruded samples were given a normalizing treatment, following the hot extrusion, in order to restore the initial grain size (Table III) to that obtained after spray deposition (Table III), and thereby provide a valid comparison; this normalizing treatment was described in the experimental section. In order to gain some insight into the effects of porosity on grain growth, the results in Tables II and III show that the presence of porosity retards grain growth in the SiC-containing material, whereas the presence of porosity either increases (400 °C) or has no significant effect (600 °C) on grain growth on unreinforced Al-Li samples exposed for more than 50 minutes. Not unexpectedly, however, a monotonic increase in grain size with temperature was noted for all samples, regardless of the presence of porosity (Tables II and III).

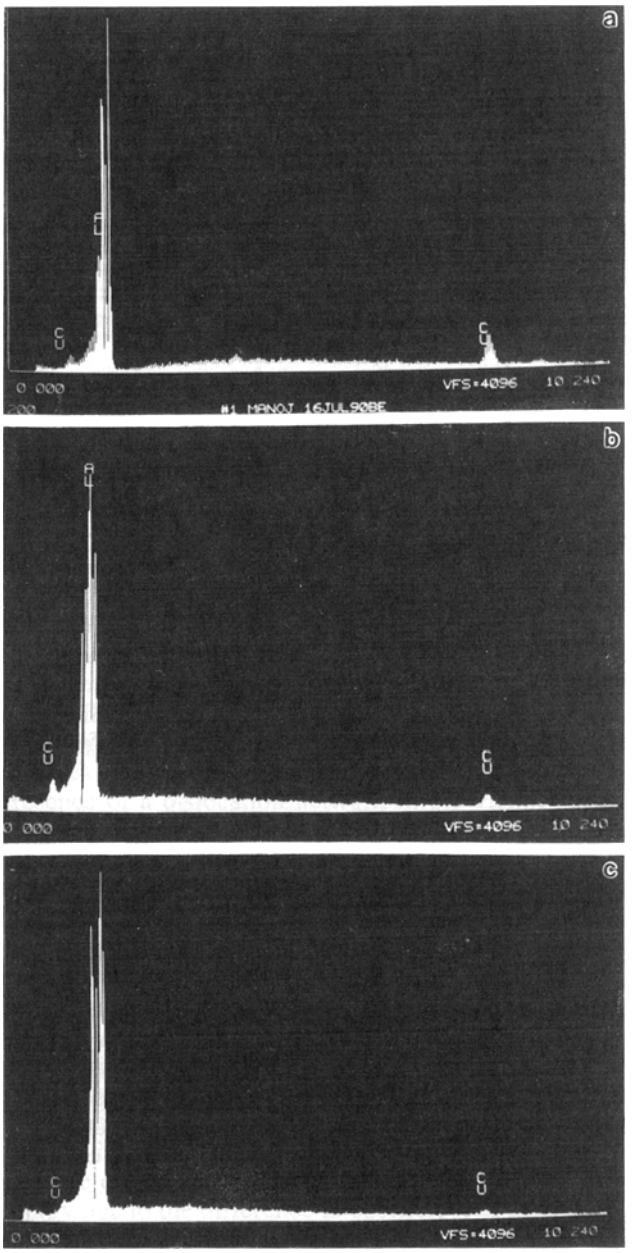

Fig. 3—Results of the EDAX point analysis conducted at various locations in the spray-deposited Al-Cu material: (*a*) inside a pore, (*b*) 2 μm from a pore, and (*c*) 6 μm from a pore.

Table II. Results of the Grain Size Measurements for Different Intervals of Time and Temperature for As-Spray Atomized and -Deposited Samples of Al-Li and Al-Li-SiC Materials

Material Time (min)	Grain Size (μm)			
	Al-Li/400 °C	Al-Li-SiC/400 °C	Al-Li/600 °C	Al-Li-SiC/600 °C
0*	75.0 ± 3.2	68.0 ± 2.2	75.0 ± 3.2	68.0 ± 2.2
1	76.0 ± 4.1	70.0 ± 2.1	140.0 ± 8.5	81.0 ± 4.5
10	79.0 ± 4.8	75.0 ± 2.4	152.0 ± 9.5	88.0 ± 4.7
50	145.0 ± 8.2	92.0 ± 2.4	230.0 ± 8.9	101.0 ± 2.8
100	175.0 ± 9.8	95.0 ± 1.4	261.0 ± 5.2	110.0 ± 8.2

*Time 0 refers to as-spray deposited grain size.

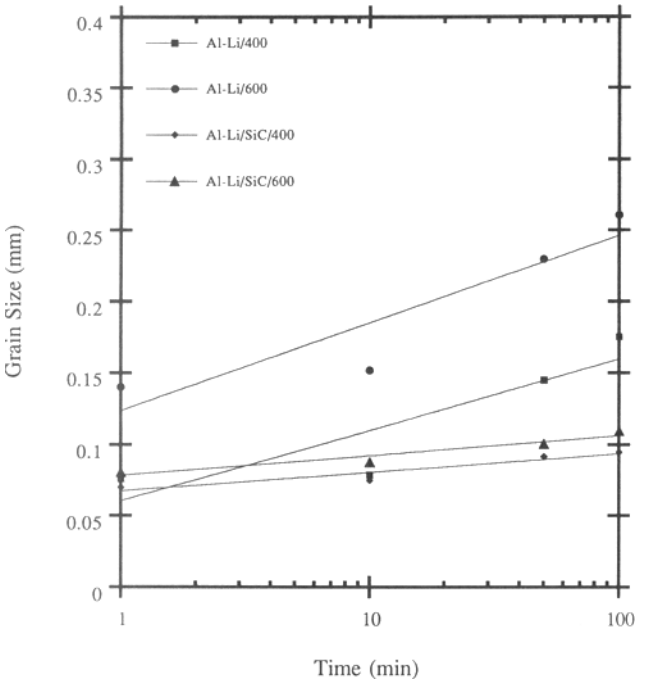

Fig. 4—Graphical representation of the logarithmic grain growth relationship observed in as-spray deposited Al-Li and Al-Li-SiC MMCs.

IV. DISCUSSION

Solid-State Cooling Effects

Once the distribution of solid, liquid, and mushy droplets impacts the deposition substrate, the newly formed grains will continue to grow during solid-state cooling. In order to gain some insight into the growth of grains in the reinforced and unreinforced materials, kinetic analysis of the data given in Table II was used in the present study to calculate the grain growth exponent. The grain growth exponent, n, represents the slope of the line

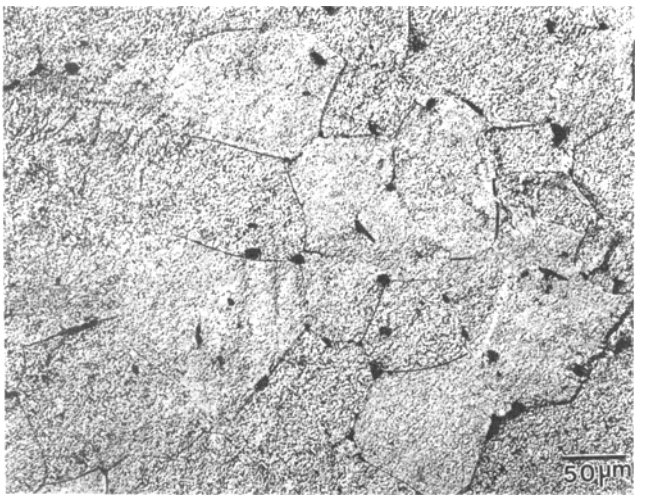

Fig. 5—Optical micrograph showing equiaxed grain morphology of a spray-deposited Al-Li sample taken from experiment 1, heat-treated at 400 °C for 100 min.

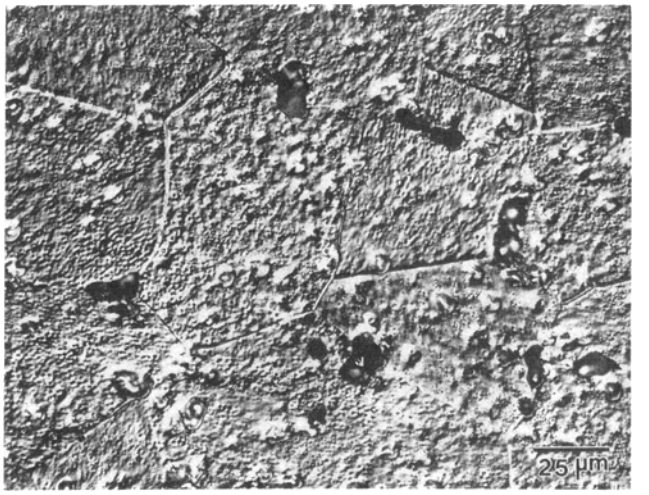

Fig. 6—Optical micrograph showing equiaxed grain morphology of the spray-deposited Al-Li-SiC sample taken from experiment 2, heat-treated at 600 °C for 100 min.

when the grain size (in millimeters) is plotted against time (in minutes) on a log-log scale.[22,23,24] The empirical relationship correlating grain size, annealing time, and grain growth exponent may be represented as

$$D = C \cdot t^n \quad [2]$$

where D is the average grain diameter, t is the annealing time, and C and n are constants. The numerical values of C and n depend on alloy composition and on annealing temperature. The values of n have been reported to range from 0.05 to 0.50; a discussion on the significance of the grain growth exponent, n, can be found elsewhere.[25,26] The main assumptions involved in the development of Eq. [2] are as follows: (a) the grains have an equiaxed morphology, (b) there is no prior deformation, and (c) the grain growth is normal.[22,23,24] Regarding the grain morphology, the presesnce of equiaxed grains has been established in a previous section. In addition, the presence of recrystallized grain morphology after hot extrusion and thermal treatment precludes any significant effects of deformation on grain growth. Finally, the linear relationship observed between grain growth and annealing time, as seen in Figure 4, provides experimental basis to the assumption of normal growth. The results of grain growth studies conducted on the as-spray deposited and extruded materials showed that this material began to exhibit abnormal grain growth behavior after extended annealing times. This is evident from the large standard deviations obtained from the grain size measurements (Table III). Therefore, no attempt was made to calculate the grain growth exponent for the extruded materials.

A few comments are in order regarding the values of grain growth exponent (n) obtained in the present study. It can be seen from Table IV that the value of the grain growth exponent (n) for a constant temperature is lower for the Al-Li-SiC material (0.065 to 0.070) relative to that of the Al-Li material (0.139 to 0.187). Furthermore, the results also show that the value of n decreases with

Table III. Results of the Grain Size Measurements for Different Intervals of Time and Temperature for Extruded Samples of Al-Li and Al-Li-SiC Materials

Material Time (min)	Grain Size (μm)			
	Al-Li/400 °C	Al-Li-SiC/400 °C	Al-Li/600 °C	Al-Li-SiC/600 °C
0*	76.0 ± 4.9	65.0 ± 2.7	76.0 ± 4.1	65.0 ± 2.7
1	80.0 ± 7.6	81.0 ± 3.2	165.0 ± 7.1	100.0 ± 5.8
10	87.0 ± 4.6	95.0 ± 6.6	207.0 ± 17.1	128.0 ± 13.4
50	99.0 ± 9.1	108.0 ± 12.4	211.0 ± 11.0	138.0 ± 10.0
100	104.0 ± 13.2	121.0 ± 3.6	251.0 ± 26.8	142.0 ± 27.3

*Time 0 refers to as-spray deposited grain size achieved after normalizing heat treatment given to the spray-deposited and extruded samples.

an increase in temperature for Al-Li and Al-Li-SiC materials. On the basis of the results of other investigators,[25,26] one would anticipate an increase in the value of n with temperature. While this anomalous behavior of the Al-Li and Al-Li-SiC materials is not clearly understood, it is thought to be related to the segregation of alloying elements to free surfaces and to the nucleation of precipitated phases (Figures 2 and 3). For example, the results of SEM/energy-dispersive analysis by X-ray (EDAX) studies shown in Figure 3 clearly suggest segregation of elemental copper to the matrix regions adjacent to the porosity. A similar analysis could not be conducted for lithium, as a result of the limitations associated with the SEM/EDAX technique to detect the elements with atomic number below 5. However, it is anticipated that the effect will be more pronounced for lithium as a result of its high diffusivity in the aluminum matrix. Regarding the effects of second-phase precipitation on grain growth, one needs to consider the composition of the binary alloy. On the basis of the binary Al-Li phase diagram and the Li composition used in the present study, precipitation of the ordered LI_2 δ' (Al_3Li) phase can be anticipated at 400 °C.[27] In addition, annealing (500 °C to 600 °C) of Al-Li alloys has been reported to result in the formation of δ (AlLi) phase at grain boundaries.[27]

A qualitative explanation for the observation that, as a result of isochronal anneals, the grain sizes for Al-Li-SiC samples are smaller than those for Al-Li may be offered as follows. The presence of SiC particulates at the grain boundaries decreases the overall free energy of the system by decreasing the available grain boundary area. Therefore, the thermodynamic driving force for the grain boundary migration in the Al-Li-SiC is decreased, relative to that present in the Al-Li matrix. The results from optical and SEM studies conducted on the as-spray deposited materials show that the SiC particulates are located both transgranularly and intragranularly within the Al-Li matrix; this is consistent with previous findings (Table I).[3] In addition to decreasing the effective grain boundary area, the presence of SiC particulates at the grain boundaries may result in a drag force on the boundary, effectively slowing grain boundary migration. Inspection of Figure 4 and Table II shows that the grain size of the Al-Li alloy exposed at 400 °C for 100 minutes was 175 μm, whereas the grain size of the Al-Li-SiC at the same temperature and time was only 95 μm. The same trend was observed at 600 °C for all exposure times (Table II). It is anticipated that at low temperatures, the dragging effect associated with the presence of SiC particulates at the grain boundaries may be enhanced by the presence of a dislocation network in the vicinity of the interface formed between the SiC particulates and the Al-Li matrix. The presence of a dislocation network at SiC/Al interfaces has been confirmed by numerous investigators[28,29] and has been proposed to develop as a result of the large difference in coefficient of thermal expansion between SiC and Al. Furthermore, the presence of a dislocation network at the SiC/Al interface will enhance solute segregation, which, in turn, will reduce the mobility of the grain boundaries. The preferential segregation of constituent elements at reinforcement/matrix interfaces has been documented by various investigators.[8,30,31] It must be noted that the presence of SiC particulates in the matrix introduces strain energy due to the difference in coefficient of thermal expansion between SiC particulates and the matrix. The strain energy thus introduced in the lattice may have an influence in retarding grain growth, as suggested in related studies,[32] and is the subject of continuing research work.

Table IV. Results of the Grain Growth Kinetic Studies

Material	n	C
Al-Li/400 °C	0.187	0.067
Al-Li/600 °C	0.139	0.129
Al-Li-SiC/400 °C	0.070	0.068
Al-Li-SiC/600 °C	0.065	0.079

Regarding the effect of porosity on grain growth, the results shown in Tables II and III suggest that the magnitude of grain size of the as-spray deposited Al-Li-SiC material is 21 to 23 pct lower than that of the as-spray deposited and extruded Al-Li-SiC material. The presence of a fine distribution of pores at the grain boundaries will have a similar effect to that of SiC, effectively slowing down grain boundary migration.[32] The results for the Al-Li material are unexpected, however, in that the data shown in Table III suggest that the presence of porosity increases the rate of grain growth after a short transient. The experimental results from Tables II and III show that the grain size of the Al-Li material with porosity at 400 °C/100 min is 46 pct higher than the corresponding grain size of the extruded material under identical conditions. This unusual behavior, analogous

to the decrease in the value of the grain growth exponent with temperature noted previously, is thought to be related to elemental segregation and to the nucleation of secondary phases and is the subject of continuing studies.

V. CONCLUSIONS

The primary conclusions that may be drawn from this work are as follows:

1. The observed decrease in grain size which results from the coinjection of ceramics during spray atomization and deposition is influenced by a decrease in grain boundary migration during solid-state cooling.
2. The sharp decrease in the rate of grain growth, observed in the present study for the SiC-containing material, suggests that the SiC effectively slows grain boundary migration. This observation is supported by kinetic analyses of the grain growth data, which showed that the values of the grain growth exponent in the 400 °C to 600 °C temperature range were 0.065 to 0.070 and 0.139 to 0.187 for the Al-Li-SiC and Al-Li materials, respectively.
3. Finally, further work is required in order to identify the role of porosity in affecting the grain growth behavior of monolithic Al-Li alloy.

ACKNOWLEDGMENTS

The authors wish to acknowledge the Army Research Office (Grant No. DAALO3-89-K-0027) for financial support; Reynolds Metals for supplying the alloys; Superior Graphite Company for supplying the SiC; Buehler Inc. for facilitating the image analysis; Mr. Irwin Sauer for his assistance with the experimental part of this study; and Lisa Rehbaum for typing the manuscript. In addition, EJL wishes to acknowledge the National Science Foundation (MSS-8957449) for financial support of his research activities. Finally, the authors would like to thank the reviewers for their many useful comments.

REFERENCES

1. M. Gupta, F.A. Mohamed, and E.J. Lavernia: *Metall. Trans. A*, 1992, vol. 23A, pp. 831-43.
2. Yue Wu: Ph.D. dissertation research, University of California–Irvine, 1991.
3. M. Gupta, F.A. Mohamed, and E.J. Lavernia: *Mater. Manuf. Processes*, 1990, vol. 5, p. 165.
4. M. Gupta, F.A. Mohamed, and E.J. Lavernia: *Proc. Int. Symp. on Advances in Processing and Characterization of Ceramic Metal Matrix Composites*, H. Mostaghaci, ed., CIM/ICM, Pergamon Press, New York, NY, Aug. 1989, vol. 17, p. 236.
5. T.C. Willis: *Met. Mater.*, 1988, vol. 4, p. 485.
6. C.L. Buhrmaster, D.E. Clark, and H.O. Smart: *J. Met.*, 1988, vol. 40, p. 44.
7. A.R.E. Singer: *Annals of the CIRP*, 1983, vol. 32, p. 145.
8. M. Gupta, F.A. Mohamed, and E.J. Lavernia: *Conf. Proc. Symp. on Fundamental Relationships Between Microstructures and Mechanical Properties of Metal Matrix Composites*, M.N. Gungor and P.K. Liaw, eds., Oct. 1–5, 1989, Indianapolis, IN, TMS Publication, Warrendale, PA, p. 3.
9. J. White, I.G. Palmer, I.R. Hughes, and S.A. Court: in *Aluminum-Lithium Alloys V*, T.H. Sanders, Jr. and E.A. Starke, Jr., eds., March 27–31, 1989, Williamsburg, VA, Materials and Component Engineering Publications Ltd., vol. 3, p. 1635.
10. K.A. Kojima, R.E. Lewis, and M.J. Kaufman: in *Aluminum-Lithium Alloys V*, T.H. Sanders, Jr. and E.A. Starke, Jr., eds., March 27–31, 1989, Williamsburg, VA, Birmingham, U.K. vol. 1, p. 85.
11. V.C. Nardone and K.W. Prewo: *Scripta Metall.*, 1986, vol. 20, p. 43.
12. K.T. Park, E.J. Lavernia, and F.A. Mohamed: *Acta Metall. Mater.*, 1990, vol. 38, p. 2.
13. R.H. Bricknell: *Metall. Trans. A*, 1986, vol. 17A, pp. 583-91.
14. H.C. Fiedler, T.F. Sawyer, R.W. Koop, and A.G. Leatham: *J. Met.*, 1987, vol. 39, p. 28.
15. E.J. Lavernia and N.J. Grant: *Mater. Sci. Eng.*, 1988, vol. 98, p. 381.
16. E.J. Lavernia and N.J. Grant: *Int. J. Rapid Solidification*, 1986, vol. 2, p. 93.
17. M. Ruhr, E.J. Lavernia, and J.C. Baram: *Metall. Trans. A*, 1990, vol. 21A, pp. 1785-89.
18. S.D. Annavarapu, D. Apelian, and A. Lawley: *Metall. Trans. A*, 1988, vol. 19A, pp. 3077-86.
19. P. Mathur, D. Apelian, and A. Lawley: *Acta Metall.*, 1989, vol. 37, p. 429.
20. E.J. Lavernia: *Int. J. Rapid Solidification*, 1989, vol. 5, p. 47.
21. Yue Wu and E.J. Lavernia: *J. Met.*, 1991, vol. 43 (8), p. 16.
22. P.A. Beck, J.C. Kremer, L.J Demer, and M.L. Holzworth: *Trans. TMS-AIME*, 1948, vol. 175, p. 372.
23. P.A. Beck: *J. Appl. Phys.*, 1948, vol. 19, p. 507.
24. P.A. Beck, J. Towers, and W.O. Manley: *Trans. TMS-AIME*, 1951, vol. 175, p. 634.
25. R.L. Fullman: *Metal Interfaces*, ASM, Cleveland, OH, 1952, p. 179.
26. P. Cotterill and P.R. Mould: *Recrystallization and Grain Growth in Metals*, Surrey University Press, Surrey, U.K., 1976, p. 275.
27. E.J. Lavernia, T.S. Srivatsan, and F.A. Mohamed: *J. Mater. Sci. Lett.*, 1990, vol. 25, p. 1137.
28. R.H. Bricknell: *Metall. Trans. A*, 1986, vol. 17A, pp. 583-91.
29. R.J. Arsenault: *Mater. Sci. Eng.*, 1984, vol. 64, p. 171.
30. M. Gupta, F.A. Mohamed, and E.J. Lavernia: *J. Mater. Sci.*, 1992, in press.
31. M. Ueki, M. Kana, and I. Okamoto: *J. Mater. Sci. Lett.*, 1986, vol. 5, p. 1261.
32. Robert E. Reed Hill: *Physical Metallurgy Principles*, D. Van Nostrand Company, Inc., p. 206.